ARTICLE
Journal of Cellular Biochemistry 111:627–633 (2010)

Journal of Cellular Biochemistry

Copper (II) Promotes the Formation of Soluble Neurotoxic PrP Oligomers in Acidic Environment

Di Wu,[1] Wentao Zhang,[1] Qingying Luo,[2] Kan Luo,[1] Liqin Huang,[1] Wenxi Wang,[1] Tao Huang,[1] Rui Chen,[1] Yi Lin,[2] Daiwen Pang,[2] and Gengfu Xiao[1,3*]

[1] *State Key Laboratory of Virology and Modern Virology Research Centre, College of Life Sciences, Wuhan University, Wuhan 430072, PR China*

[2] *College of Chemistry and Molecular Science, Wuhan University, Wuhan 430072, PR China*

[3] *State Key Laboratory of Virology, Wuhan Institute of Virology, Chinese Academy of Sciences, Wuhan 430071, PR China*

ABSTRACT

Prion diseases are classically considered to be ''amyloid diseases'' caused by the deposition of amyloid fibrils in the brain. Recent studies identified soluble oligomers of PrP (prion protein) in damaged neuronal tissue. However, the details of PrP oligomerization are still unclear. In this study, we demonstrate that Cu^{2+} plays a vital role in the formation of soluble PrP oligomers. A Cu^{2+}-triggered structural conversion of PrP (90–231) to a β-sheet isoform in pH 5.0 buffer was revealed by circular dichroism spectra and fluorescence measurement. Soluble oligomers were isolated by size exclusion chromatography from experimental solutions, allowing atomic force microscopy to reveal their morphology. 3-(4,5-Dimethylthiazol-2-yl)-2,5-diphenyltetrazolium bromide (MTT) and flow cytometry assays demonstrated that oligomeric PrP induced significant damage in and apoptosis of neuroblastoma SK-N-SH cells. These results indicate that in an acidic environment, Cu^{2+} promotes the formation of neurotoxic soluble PrP oligomers. J. Cell. Biochem. 111: 627–633, 2010.

KEY WORDS: PRION; OLIGOMER; COPPER; ACIDIC PH; TOXICITY

Neurodegenerative disorders, including Alzheimer's, Parkinson's, and Prion diseases, are classically considered to be ''amyloid diseases'' caused by the deposition of amyloid fibrils in the brain. However, recent works have argued that early neuronal damage is related to the formation of soluble oligomers, or protofibrils, of amyloidogenic proteins [Caughey and Lansbury, 2003; Kayed et al., 2003; Walsh and Selkoe, 2004]. Prion diseases are initiated by the conversion of cellular PrP (PrP^{C}) to a pathogenic isoform (PrP^{Sc}) [Prusiner, 1998]. Interestingly, the 300–600 kDa non-fibrillar particles are the most efficient initiators of transmissible spongiform encephalopathy (TSE) disease [Silveira et al., 2005]. Soluble subfibrillar oligomers of amyloidogenic peptide or protein may induce neuron impairment, whereas the formation of large amyloid fibrils, which act like innocuous protein deposits, could be protective [Caughey and Lansbury, 2003]. However, the details of the process by which soluble PrP oligomers are derived from native-state PrP are still unclear.

Previous studies have shown that the transition of PrP from its native state to soluble oligomers is a pH-dependent process [Gerber et al., 2008]. The conformational transition from the native monomeric PrP to soluble oligomers occurs at an acidic pH. Moreover, it appears that acidic conditions favor the existence of soluble PrP oligomers [Baskakov et al., 2002].

It is widely accepted that PrP specifically binds Cu^{2+} and may function as a cuproprotein in vivo [Hornshaw et al., 1995; Whittal et al., 2000; Qin et al., 2002]. Accumulating evidence indicates that Cu^{2+} is able to modulate the pathogenesis of prion disease in vivo [Pattison and Jebbett, 1971; Brown et al., 1997; Hijazi et al., 2003; Sigurdsson et al., 2003] at physiological concentrations of 10–20 μM. However, the role of Cu^{2+} in PrP oligomerization has not been investigated. Here, the recombinant PrP (90–231) was refolded and we illustrated that Cu^{2+} is a vital factor involved in the formation of neurotoxic soluble PrP oligomers at low pH. The experimental pH of pH 5.0 was chosen to mimic the acidic

Grant sponsor: National Key Scientific Program (973)-Nanoscience and Nanotechnology; Grant number: 2006CB933100; Grant sponsor: Program for New Century Excellent Talents in University; Grant number: NCET-06-0620; Grant sponsor: Program for Changjiang Scholars and Innovative Research Team in University; Grant number: IRT 0745; Grant sponsor: MOE for PhD program; Grant number: 20060486025.

*Correspondence to: Prof. Gengfu Xiao, Wuhan Institute of Virology, Chinese Academy of Sciences, Xiaohongshan 44, Wuchang, Wuhan 430071, PR China. E-mail: xiaogf@wh.iov.cn

Received 15 March 2010; Accepted 3 June 2010 • DOI 10.1002/jcb.22743 • © 2010 Wiley-Liss, Inc.
Published online 18 June 2010 in Wiley Online Library (wileyonlinelibrary.com).

environment within late endosomes. Our results indicated that in an acidic environment, physiological Cu^{2+} concentrations may enhance the generation of neurotoxic PrP oligomers.

MATERIALS AND METHODS

PLASMID CONSTRUCTIONS

The widely used [Baskakov et al., 2002] human PrP gene (encoding residues 90–231), was amplified by polymerase chain reaction (PCR) using human genomic DNA templates. The primers were 5′-CCAAGT-TCATATGGGTCAAGGAGGTGGCAC-3′ (forward sequence) and 5′-TAAGAGCTCGAGGCTCGATCCTCTCTGG-3′ (reverse sequence). The PCR product was cloned into the *Nde*I and *Xho*I sites of the vector pET30a (+).

EXPRESSION AND PURIFICATION OF RECOMBINANT HUMAN PRP (90–231)

The purification and refolding process was carried out on a nickel ion-charged sepharose column (Amersham Biosciences). Briefly, freshly transformed BL21 (DE3) *Escherichia coli* containing the plasmid pET-PrP (90–231) were transferred to 1 L Luria–Bertani (LB) medium supplemented with 50 μg/ml kanamycin at 37°C until the OD reached 1.0, at which point protein expression was induced for 6 h using 1 mM isopropyl β-D-thiogalactoside. Bacteria were harvested by centrifugation at 4,000*g* for 15 min at 4°C, resuspended in 20 mM Tris/HCl (pH 8.0), 150 mM NaCl, 0.1 mM PMSF, 1 mg/ml lysozyme, and incubated at 21°C for 2 h before further lysis by sonication. Samples were centrifuged at 13,000*g* for 20 min. The protein pellets were extensively washed using 1% Triton X-100, 2 M NaCl, and 2 M urea and resuspended in 20 mM Tris/HCl (pH 8.0), 6 M Gdn-HCl, and 10 mM 2-mercaptoethanol. The inclusion bodies were purified and refolded on a nickel ion-charged sepharose column by decreasing Gdn-HCl gradient concentrations. Finally, PrP was eluted by 50 mM sodium acetate.

SOLUBLE OLIGOMER PREPARATION

Recombinant PrP (90–231) was incubated at 65°C for 2 h with 20 μM Cu^{2+}. Solutions were buffered with 80 mM sodium phosphate at pH 5.0. The concentration of PrP was 0.3 mg/ml (20 μM). Controls with PrP alone in buffer without copper ions were incubated simultaneously.

CIRCULAR DICHROISM

Far-UV (190–250 nm) CD spectra were measured on a JASCO J-810 spectro-polarimeter using 1-mm path length quartz cuvettes, scanning at 100 nm/min, with a bandwidth of 2 nm and data spacing of 1 nm. Each spectrum represents the average of two individual scans after subtracting the background spectra.

FLUORESCENT DYE BINDING

The fluorescence of bis-ANS (4,4′-bis(1-anilinona-phthalene 8-sulfonate), Sigma) was monitored at 475 nm (excitation at 385 nm; excitation slit was 10 nm; emission slit was 10 nm; 1 cm rectangular cuvettes). ANS (10 μM) mixed with 0.5 μM PrP (90–231) was incubated for 15 min at room temperature before monitoring fluorescence. Background fluorescence was subtracted from the results.

SIZE-EXCLUSION CHROMATOGRAPHY

All separations were performed at 25°C with a flow rate of 1 ml/min using a Waters Biosuite HR 250 SEC HPLC gel filtration column (300 mm × 7.80 mm) equilibrated with running buffer containing 80 mM sodium phosphate (pH 5.0).

ATOMIC FORCE MICROSCOPY

AFM imaging was conducted with a PicoScan atomic force microscope (Molecular Imaging, USA). Approximately 10 μl of diluted sample solution (ca. 0.03 mg/ml) was dropped onto freshly cleaved ruby muscovite mica substrate (Digital Instruments, USA). After 5 min, the mica surface was rinsed with ultrapure water (18.2 MΩ, Millipore) and gently blown dry with nitrogen. Freshly prepared samples were mounted on the AFM stage and imaged in MAC mode at 25°C using MAClever Type II probes (spring constant = 2.8 N/m, resonant frequency = ~85 kHz; Molecular Imaging). Scan rates were 1–2 Hz. The images were rastered at 256 × 256 pixels, unfiltered and flattened when needed.

CELL CULTURES

Human SK-N-SH neuroblastoma cells (China Center for Type Culture Collection, CCTCC) were cultured in minimum essential medium (Hyclone, USA) supplemented with 10% fetal bovine serum (Gibco, USA). Cultured cells were grown at 37°C in a humidified atmosphere containing 5% CO_2.

MTT REDUCTION ASSAY

Cells were plated onto a 96-well plate at a density of 8,000 cells per well in 200 μl of fresh minimum essential medium with 10% fetal bovine serum. After 24 h, 50 μl of samples and controls was added to the wells with 150 μl fresh medium. Cell viability was evaluated 24 h later by the MTT reduction assay. A volume of 10 μl of a 5.5 mg/ml stock of MTT in PBS was added to each well and incubated for 4 h. The reaction was terminated by adding *N*,*N*′-dimethylformamide. Production of blue formazan crystals by dehydrogenase enzymes and flavin oxidases was measured by recording absorbance values at 570 nm.

FLOW CYTOMETRY ANALYSIS

Cell apoptosis was characterized by flow cytometry, assessing annexin V- and propidium iodide-positive cells. Cells were plated onto a 12-well plate, and 250 μl of samples or controls was added into the wells with 750 μl medium. After 12 h stimulation, cells were harvested and washed with PBS. Cells were stained with annexin V and propidium iodide (PI) (rh Annexin V/FITC Kit, Bender Medsystem, Austria) and analyzed by flow cytometry to assess the proportion of apoptotic and non-viable cells, respectively.

RESULTS

CU^{2+} PROMOTES THE CONVERSION OF RECOMBINANT PRP (90–231) TO A β-SHEET STRUCTURE IN SOLUTION

In this study, we refolded recombinant PrP (90–231) purified from inclusion bodies into a monomeric α-helical structure. The protein was incubated at 65°C, which is considered to be the T_m for the C-terminal globular domain and should generate a partially denatured

state that might be more aggregate-prone [Martins et al., 2006]. Meanwhile, 20 μM Cu^{2+} was also added to the buffers. The experiments were carried out at pH 5.0 to mimic the acidic environment of late endosomes, which have been implicated as the intracellular compartment where the conformational transition of PrP^C may take place [Caughey and Raymond, 1991; Borchelt et al., 1992]. After incubation, the protein remained in solution.

In order to define the alterations in secondary PrP structure induced by our experimental conditions, we monitored their far-UV CD spectra. Refolded PrP showed typical features of a protein containing significant α-helical structure with well-defined minima at 208 and 222 nm. After a 2-h incubation with Cu^{2+}, the negative bands around 208 and 222 nm decreased, which is indicative of a substantial increase in β-sheet structure, whereas the PrP in control experiments incubated without Cu^{2+} had no noticeable conformational changes (Fig. 1a). The far-UV CD signal at 222 nm was also continuously recorded. In contrast to the control group, the negative signals of PrP incubated with Cu^{2+} decreased much faster, indicating that Cu^{2+} promoted the changes in PrP conformation (Fig. 1b).

To further characterize the structural transition of PrP, we used Bis-ANS, an environment-sensitive fluorescent dye whose fluorescence emission increases dramatically upon exposure to hydrophobic domains in proteins. It is noteworthy that during incubation, bis-ANS emission in the Cu^{2+}-containing group increased significantly compared to the control groups, which are in agreement with our CD results (Fig. 1c).

After incubation at pH 5.0, PrP remained in solution. However, the same incubations were carried out in pH 6.0 and 7.0 conditions. Coupled with the observed structural alterations, deposits appeared in higher pH conditions. ThT was used to determine whether these accumulations were amyloid fibrils, but no emission was observed (data were not shown). It is possible that these PrPs may form amorphous accumulations.

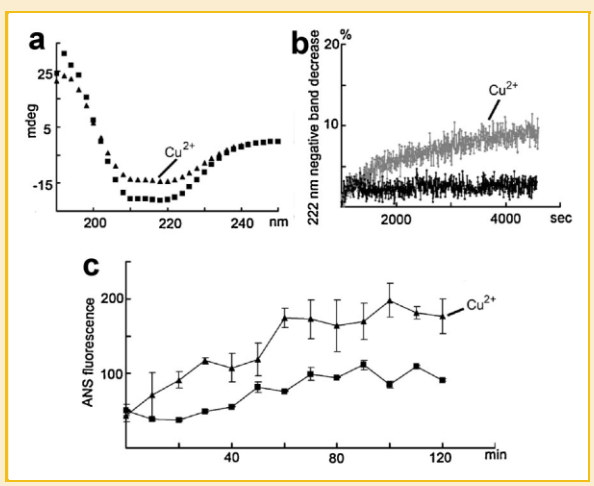

Fig. 1. Structural changes monitored by circular dichroism (CD) and fluorescence. a: CD spectra at pH 5.0 after 2 h incubation at 65°C in buffers with (▲) or without (■) Cu^{2+}. b: Continuous CD signals at 222 nm during 2 h incubation in buffers with (gray) or without (black) Cu^{2+}. c: Bis-ANS fluorescence of PrP during 2 h incubation at 65°C in buffer with (▲) or without (■) Cu^{2+}.

SOLUBLE OLIGOMERS IDENTIFIED BY HIGH-PERFORMANCE LIQUID CHROMATOGRAPHY (HPLC) AND ATOMIC FORCE MICROSCOPE (AFM)

High-performance liquid chromatography (HPLC) was used to identify whether soluble accumulations formed under our experimental conditions. Figure 2 shows the size exclusion chromatographic pattern of incubated PrP on a Waters Biosuite HR 250 SEC HPLC gel filtration column. The 16 kDa monomeric native PrP eluted at 9.7 ml (Fig. 2a), whereas oligomers eluted at 5.6 ml (Fig. 2b). The oligomers corresponded to a molecular size of about 500 kDa. As the incubation continued, a decrease in the monomeric population coincided with the growth of the oligomeric population. After 2 h of incubation at pH 5.0 with Cu^{2+}, oligomers predominated, but no oligomers could be detected in controls (Fig. 2c).

The morphology of PrP monomers and oligomers was studied by AFM. After incubation, PrP buffered with or without Cu^{2+} was analyzed. PrP incubated without Cu^{2+} appeared monomeric and had an average diameter of 15 ± 2 nm (Fig. 3a). Particles with an average diameter of 39 ± 7 nm (Fig. 3b) corresponded to the oligomers promoted by Cu^{2+}. Additionally, the oligomers were homogeneous and well dispersed, with a large eyeshot image shown in Figure 3c.

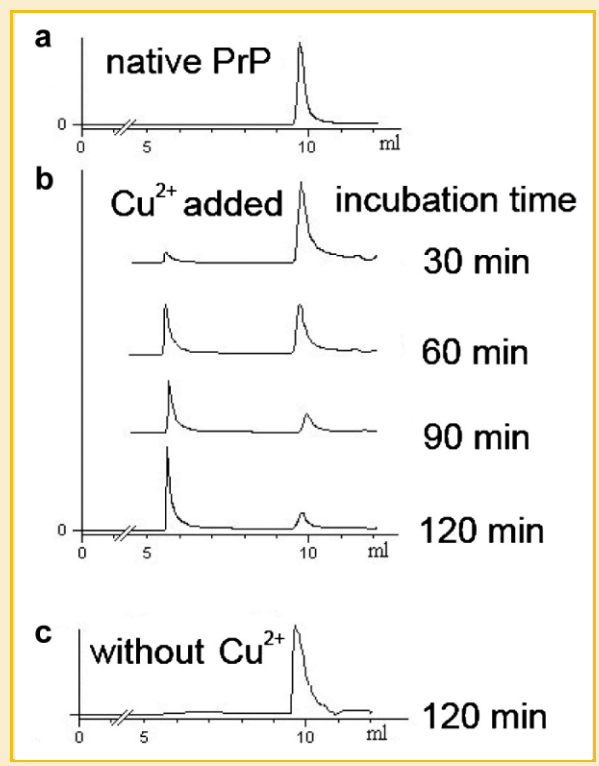

Fig. 2. Soluble oligomers separated by size-exclusion chromatography (SEC). SEC showed the formation of soluble oligomers. a: Peak of monomeric native PrP. b: The peaks of oligomers incubated for 30, 60, 90, and 120 min at pH 5.0 with Cu^{2+}. c: PrP incubated for 120 min at pH 5.0 without Cu^{2+}.

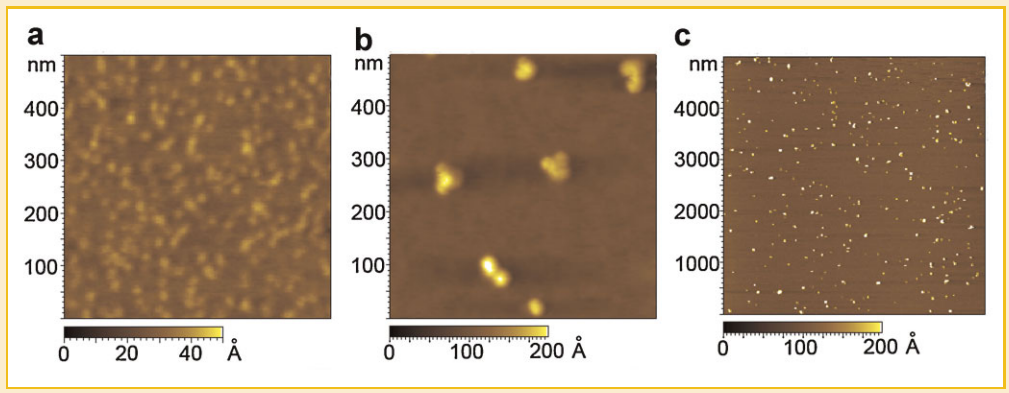

Fig. 3. Morphology of PrP oligomers detected by atomic force microscopy (AFM). a: Morphology of monomeric PrP incubated at pH 5.0 without Cu^{2+}. b: PrP oligomer incubated for 2 h at pH 5.0 with Cu^{2+}. c: A larger eyeshot of panel b. [Color figure can be viewed in the online issue, which is available at wileyonlinelibrary.com.]

Both the HPLC and AFM results confirmed that Cu^{2+} was a pivotal factor in the formation of PrP soluble oligomers.

PRP SOLUBLE OLIGOMERS WERE CYTOTOXIC TO NEUROBLASTOMA CELLS AND INDUCED APOPTOSIS

The toxicity of the soluble oligomers was studied using human SK-N-SH neuroblastoma cells. Cell viability was measured by MTT reduction assay, which is commonly used for assessing cell survival in the presence of protein aggregates [James et al., 1997; Abe and Saito, 1998]. Student's *t*-test was performed to compare the cells exposed to PrP incubations and their buffers only.

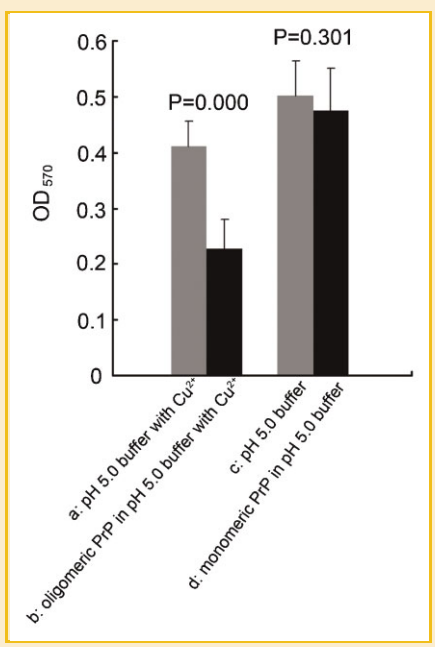

Fig. 4. Cell viability measured by MTT. Toxic effects of PrP incubated under each condition were tested. Absorbance values at 570 nm of cells exposed to: (a) pH 5.0 buffers with Cu^{2+}, (b) PrP oligomers in pH 5.0 buffers with Cu^{2+}, (c) pH 5.0 buffer without Cu^{2+}, (d) monomeric PrP in pH 5.0 buffer without Cu^{2+}. *t*-Tests were performed to analyze whether the cytotoxicity of incubated PrPs was significant when compared with the corresponding buffers (a with b, c with d). Respective *P*-values were shown.

The viability of the group exposed to soluble PrP oligomers (Fig. 4b) decreased by 44% ($P = 0.000$) compared to control buffer containing Cu^{2+} (Fig. 4a). However, there was no significant statistical differences between monomeric PrP (Fig. 4d) and its control (Cu^{2+}-free) buffer (Fig. 4c; $P > 0.05$), suggesting that monomeric PrP is not toxic to neuroblastoma cells. Although Cu^{2+} alone indeed showed some toxicity, these results indicate that soluble oligomers derived from incubations with Cu^{2+} are highly toxic to the cultured cells according to the comparison.

Cell apoptosis was monitored by assessing annexin V- and propidium iodide-positive cells by flow cytometry. Normal cell cultures showed early apoptosis in only about 5% of cells (Fig. 5a). Proportions of apoptotic cells in cultures exposed to buffer containing Cu^{2+} only or with added native PrP rose slightly to about 10% (Fig. 5b,c), whereas the proportion of apoptotic cells in oligomer-treated cultures reached 31.9% (Fig. 5d). Taken together, our data strongly suggest that the soluble oligomers generated by Cu^{2+} are toxic to cultured neuroblastoma cells and induced apoptosis. This study also provides evidence that oligomers derived from recombinant PrP (90–231) possess significant cytotoxicity.

DISCUSSION

Data accumulated over the last few years indicated that soluble oligomers are toxic species that damage the cell in neurodegenerative diseases [Bucciantini et al., 2002, 2004]. Certain non-amyloidal oligomeric forms of PrP have been demonstrated to be cytotoxic as well [Caughey and Lansbury, 2003; Silveira et al., 2005; Vasan et al., 2006]. The oligomerization of PrP may be a key step in prion pathogenesis, but the details of this process remain unclear.

Previous studies indicated that the transition of native-state PrPs into soluble oligomers is a pH-dependent process [Gerber et al., 2008] and that soluble oligomers could be generated under acidic conditions similar to those observed in endocytic vesicles [Baskakov et al., 2002]. Naturally occurring PrP^{C} or PrP^{Sc} is internalized and passes through endocytic pathways [Campana et al., 2005]. The pH

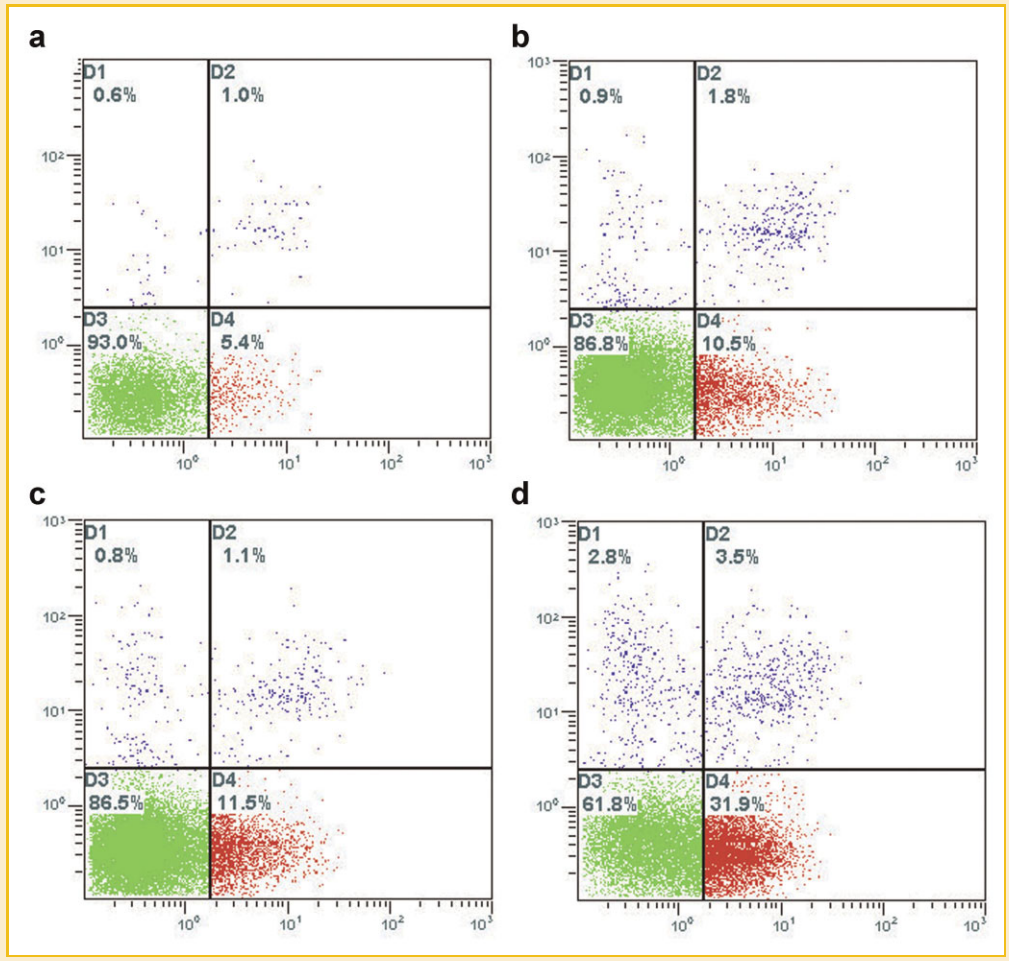

Fig. 5. Cell apoptosis detected by flow cytometry. Flow cytometry analysis used to detect annexin V-FITC and propidium iodide-positive cells. The *x*-axis shows the fluorescent intensity of FITC, and the *y*-axis shows the fluorescent intensity of propidium iodide. D4 denotes early apoptosis. D2 denotes late apoptosis. Normal and dead cells are contained in D3 and D1, respectively. a: Control cells. b: Cultures exposed to pH 5.0 buffers containing Cu^{2+}. c: Cultures exposed to pH 5.0 buffers containing Cu^{2+} with native PrP. d: Cultures exposed to PrP oligomers formed in pH 5.0 buffers containing Cu^{2+} displayed significant apoptosis. [Color figure can be viewed in the online issue, which is available at wileyonlinelibrary.com.]

in the endocytic pathway gradually becomes acidic, reaching a pH of about 5 in the late endosome. Indeed, the endosomal–lysosomal system (ELS) has been suggested to play a role in the pathogenesis of prion diseases [Kovacs et al., 2007]. In this study, we chose a pH of 5.0 to mimic the acidic environment within late endosomes and our results were consistent with earlier studies indicating that an acidic pH favors the generation of soluble oligomers.

In traditional opinion, the four histidine-containing octarepeats region of the PrP located between residues 60 and 91 was the major Cu^{2+} binding sites on PrP, while over last few years accumulated researches indicated that histidyl residues 96 and 111 the so-called "fifth site" on PrP play important roles in binding Cu^{2+} [Berti et al., 2007; Osz et al., 2007; Klewpatinond et al., 2008]. Copper ions are even preferentially coordinated by His96 and His111 in the unstructured amyloidogenic region of the prion protein between residues 90 and 120 [Jones et al., 2004; Osz, 2008; Viles et al., 2008; Di Natale et al., 2009]. Previous study suggested that PrP (90–231) might be more prone to chemical modification, and Cu^{2+} binding to the His96 and His111 residues can induce localized β-sheet structure [Nadal et al., 2007; Pushie et al., 2009]. The region of PrP located between 90 and 120 residues is also an important Cu^{2+} binding site and strongly affects the structure of PrP, so we focused on the interaction of Cu^{2+} and this truncated PrP (90–231). Additionally, the truncated PrP molecule has been widely used and is simpler to handle [Baskakov et al., 2002; Cobb et al., 2007].

Additionally, our study confirms that Cu^{2+} promotes the formation of soluble neurotoxic PrP oligomers. We demonstrated a Cu^{2+}-dependent secondary structure transition of PrP (90–231) into soluble oligomers with a molecular size of about 500 kDa. PrP specifically binds Cu^{2+} and may function as a cuproprotein in vivo. Furthermore, Cu^{2+} is an important cofactor involved in modulating the pathogenesis of prion disease [McKenzie et al., 1998; Hijazi et al., 2003; Sigurdsson et al., 2003]. Studies have also indicated that copper induces changes in the structure of PrP [Stockel et al., 1998] and converts the cellular prion protein into a protease-resistant species [Quaglio et al., 2001]. However, there is still debate over the role of Cu^{2+} in prion pathogenesis. Meanwhile, the relationship between copper and soluble PrP oligomers remains a mystery.

Our results confirmed that Cu^{2+} could induce the conversion of PrP (90–231) into its β-isoform and induce native PrP to assemble into neurotoxic soluble oligomers. These data appear to highlight a role for copper in modulating the pathogenesis of prion disease.

In an acidic environment, copper binding also changes following the protonation of histidyl residues. The nitrogen donor atoms of histidyl residues in imidazole are the exclusive metal-binding sites when pH falls below 5.5, favoring macrochelate structure formation [Osz et al., 2007]. Our results suggest that Cu^{2+} is a key factor involved in the formation of soluble PrP oligomers in addition to low pH. This change in ion binding at low pH might affect the construction of PrP and promote the transition to and stabilization of soluble oligomers. In vivo, PrP is internalized through endocytosis. We propose that when PrP binds excessive Cu^{2+}, the endocytic pathway becomes the primary site of PrP oligomerization and accumulation. We suggest that elevated levels of environmental Cu^{2+} increase the risk of neurodegenerative disorders caused by prions and that the ELS may be the primary site of disease pathology.

Protein conformational diseases tend to have similar pathogenesis. Our results may highlight the relationship between metal ions and prion oligomerization and might also offer insights as to the pathogenesis of other protein conformational diseases such as Alzheimer's disease (AD) and Parkinson's disease (PD).

ACKNOWLEDGMENTS

This work was supported by National Key Scientific Program (973)-Nanoscience and Nanotechnology (No. 2006CB933100), Program for New Century Excellent Talents in University (NCET-06-0620), Program for Changjiang Scholars and Innovative Research Team in University (No. IRT 0745), and grants from MOE for PhD Program (20060486025).

REFERENCES

Abe K, Saito H. 1998. Amyloid beta protein inhibits cellular MTT reduction not by suppression of mitochondrial succinate dehydrogenase but by acceleration of MTT formazan exocytosis in cultured rat cortical astrocytes. Neurosci Res 31:295–305.

Baskakov IV, Legname G, Baldwin MA, Prusiner SB, Cohen FE. 2002. Pathway complexity of prion protein assembly into amyloid. J Biol Chem 277:21140–21148.

Berti F, Gaggelli E, Guerrini R, Janicka A, Kozlowski H, Legowska A, Miecznikowska H, Migliorini C, Pogni R, Remelli M, Rolka K, Valensin D, Valensin G. 2007. Structural and dynamic characterization of copper(II) binding of the human prion protein outside the octarepeat region. Chemistry 13:1991–2001.

Borchelt DR, Taraboulos A, Prusiner SB. 1992. Evidence for synthesis of scrapie prion proteins in the endocytic pathway. J Biol Chem 267:16188–16199.

Brown DR, Qin K, Herms JW, Madlung A, Manson J, Strome R, Fraser PE, Kruck T, von Bohlen A, Schulz-Schaeffer W, Giese A, Westaway D, Kretzschmar H. 1997. The cellular prion protein binds copper in vivo. Nature 390: 684–687.

Bucciantini M, Giannoni E, Chiti F, Baroni F, Formigli L, Zurdo J, Taddei N, Ramponi G, Dobson CM, Stefani M. 2002. Inherent toxicity of aggregates implies a common mechanism for protein misfolding diseases. Nature 416: 507–511.

Bucciantini M, Calloni G, Chiti F, Formigli L, Nosi D, Dobson CM, Stefani M. 2004. Prefibrillar amyloid protein aggregates share common features of cytotoxicity. J Biol Chem 279:31374–31382.

Campana V, Sarnataro D, Zurzolo C. 2005. The highways and byways of prion protein trafficking. Trends Cell Biol 15:102–111.

Caughey B, Lansbury PT. 2003. Protofibrils, pores, fibrils, and neurodegeneration: Separating the responsible protein aggregates from the innocent bystanders. Annu Rev Neurosci 26:267–298.

Caughey B, Raymond GJ. 1991. The scrapie-associated form of PrP is made from a cell surface precursor that is both protease- and phospholipase-sensitive. J Biol Chem 266:18217–18223.

Cobb NJ, Sonnichsen FD, McHaourab H, Surewicz WK. 2007. Molecular architecture of human prion protein amyloid: A parallel, in-register beta-structure. Proc Natl Acad Sci USA 104:18946–18951.

Di Natale G, Osz K, Nagy Z, Sanna D, Micera G, Pappalardo G, Sovago I, Rizzarell E. 2009. Interaction of copper(II) with the prion peptide fragment HuPrP (76–114) encompassing four histidyl residues within and outside the octarepeat domain. Inorg Chem 48:4239–4250.

Gerber R, Tahiri-Alaoui A, Hore PJ, James W. 2008. Conformational pH dependence of intermediate states during oligomerization of the human prion protein. Protein Sci 17:537–544.

Hijazi N, Shaked Y, Rosenmann H, Ben-Hur T, Gabizon R. 2003. Copper binding to PrP^{C} may inhibit prion disease propagation. Brain Res 993:192–200.

Hornshaw MP, McDermott JR, Candy JM, Lakey JH. 1995. Copper binding to the N-terminal tandem repeat region of mammalian and avian prion protein: Structural studies using synthetic peptides. Biochem Biophys Res Commun 214:993–999.

James TL, Liu H, Ulyanov NB, Farr-Jones S, Zhang H, Donne DG, Kaneko K, Groth D, Mehlhorn I, Prusiner SB, Cohen FE. 1997. Solution structure of a 142-residue recombinant prion protein corresponding to the infectious fragment of the scrapie isoform. Proc Natl Acad Sci USA 94:10086–10091.

Jones CE, Abdelraheim SR, Brown DR, Viles JH. 2004. Preferential Cu^{2+} coordination by His96 and His111 induces beta-sheet formation in the unstructured amyloidogenic region of the prion protein. J Biol Chem 279:32018–32027.

Kayed R, Head E, Thompson JL, McIntire TM, Milton SC, Cotman CW, Glabe CG. 2003. Common structure of soluble amyloid oligomers implies common mechanism of pathogenesis. Science 300:486–489.

Klewpatinond M, Davies P, Bowen S, Brown DR, Viles JH. 2008. Deconvoluting the Cu^{2+} binding modes of full-length prion protein. J Biol Chem 283: 1870–1881.

Kovacs GG, Gelpi E, Strobel T, Ricken G, Nyengaard JR, Bernheimer H, Budka H. 2007. Involvement of the endosomal-lysosomal system correlates with regional pathology in Creutzfeldt-Jakob disease. J Neuropathol Exp Neurol 66:628–636.

Martins SM, Frosoni DJ, Martinez AM, De Felice FG, Ferreira ST. 2006. Formation of soluble oligomers and amyloid fibrils with physical properties of the scrapie isoform of the prion protein from the C-terminal domain of recombinant murine prion protein mPrP-(121-231). J Biol Chem 281:26121–26128.

McKenzie D, Bartz J, Mirwald J, Olander D, Marsh R, Aiken J. 1998. Reversibility of scrapie inactivation is enhanced by copper. J Biol Chem 273:25545–25547.

Nadal RC, Abdelraheim SR, Brazier MW, Rigby SE, Brown DR, Viles JH. 2007. Prion protein does not redox-silence Cu^{2+}, but is a sacrificial quencher of hydroxyl radicals. Free Radic Biol Med 42:79–89.

Osz K. 2008. A new, model-free calculation method to determine the coordination modes and distribution of copper(II) among the metal binding sites of multihistidine peptides using circular dichroism spectroscopy. J Inorg Biochem 102:2184–2195.

Osz K, Nagy Z, Pappalardo G, Di Natale G, Sanna D, Micera G, Rizzarelli E, Sovago I. 2007. Copper(II) interaction with prion peptide fragments encompassing histidine residues within and outside the octarepeat domain: Speciation, stability constants and binding details. Chemistry 13:7129–7143.

Pattison IH, Jebbett JN. 1971. Histopathological similarities between scrapie and cuprizone toxicity in mice. Nature 230:115–117.

Prusiner SB. 1998. Prions. Proc Natl Acad Sci USA 95:13363–13383.

Pushie MJ, Rauk A, Jirik FR, Vogel HJ. 2009. Can copper binding to the prion protein generate a misfolded form of the protein? Biometals 22:159–175.

Qin K, Yang Y, Mastrangelo P, Westaway D. 2002. Mapping Cu(II) binding sites in prion proteins by diethyl pyrocarbonate modification and matrix-assisted laser desorption ionization-time of flight (MALDI-TOF) mass spectrometric footprinting. J Biol Chem 277:1981–1990.

Quaglio E, Chiesa R, Harris DA. 2001. Copper converts the cellular prion protein into a protease-resistant species that is distinct from the scrapie isoform. J Biol Chem 276:11432–11438.

Sigurdsson EM, Brown DR, Alim MA, Scholtzova H, Carp R, Meeker HC, Prelli F, Frangione B, Wisniewski T. 2003. Copper chelation delays the onset of prion disease. J Biol Chem 278:46199–46202.

Silveira JR, Raymond GJ, Hughson AG, Race RE, Sim VL, Hayes SF, Caughey B. 2005. The most infectious prion protein particles. Nature 437:257–261.

Stockel J, Safar J, Wallace AC, Cohen FE, Prusiner SB. 1998. Prion protein selectively binds copper(II) ions. Biochemistry 37:7185–7193.

Vasan S, Mong PY, Grossman A. 2006. Interaction of prion protein with small highly structured RNAs: Detection and characterization of PrP-oligomers. Neurochem Res 31:629–637.

Viles JH, Klewpatinond M, Nadal RC. 2008. Copper and the structural biology of the prion protein. Biochem Soc Trans 36:1288–1292.

Walsh DM, Selkoe DJ. 2004. Oligomers on the brain: The emerging role of soluble protein aggregates in neurodegeneration. Protein Pept Lett 11:213–228.

Whittal RM, Ball HL, Cohen FE, Burlingame AL, Prusiner SB, Baldwin MA. 2000. Copper binding to octarepeat peptides of the prion protein monitored by mass spectrometry. Protein Sci 9:332–343.